Non-intercepting Optical Diffraction Radiation Diagnostics at ASTA

Alex H. Lumpkin
FNAL
August 20, 2012

ABSTRACT

Optical diffraction radiation (ODR) imaging has been proposed as a non-intercepting beam-size monitor for the high-power electron beams in the Advanced Superconducting Test Accelerator (ASTA) facility at FNAL. Potentially the technique would be used for the high-energy end at 500-1500 MeV. The application is evaluated in relation to successful experiments done at JLAB at 4.5 GeV with visible-light, near-field ODR detected by a standard CCD camera and the proof of principle at FLASH at 900 MeV with a 16-bit cooled CCD. The lower gamma beams of ASTA compared to JLAB will push the technology implementation towards the IR and the use of an ICCD and/or 16-bit camera.

INTRODUCTION

Characterization of the high-power electron beams of the ASTA/NML facility at FNAL will be an important aspect of demonstrating the superconducting rf (SCRF) accelerator as a test bed for technology [1]. Beam size, position, divergence, emittance, and bunch length measurements are all of interest. Previously, the feasibility of using a non-intercepting (NI) technique based on near-field optical diffraction radiation (ODR) was assessed, and two experiments at other facilities were proposed and executed in the interim [2]. Due to the projected high beam power at ASTA with 3000 micropulses of up to 3 nC each in a macropulse at 5 Hz at eventually up to 1500 MeV, the need for NI diagnostics is obvious. Although beam position is readily addressed with standard rf beam position monitors (BPMs), the transverse size and hence emittance are less easily monitored noninterceptively in a linear transport system. Besides an expensive laser-wire system, one of the few viable solutions appears to be the use of ODR [1-10] which is emitted when a charged-particle beam passes near a metal-vacuum interface. Appreciable radiation is emitted when the distance of the beam to the screen edge (impact parameter) $b \sim \gamma\lambda/2\pi$, where γ is the Lorentz factor and λ is the observation wavelength. The first near-field imaging experiments at the Advanced Photon Source (APS) with 7-GeV beams used an impact parameter of 1.25 mm from a single edge of a plane as compared to the scaling factor of ~1.4 mm (with an assumed operating wavelength of 0.628 µm) [7]. The near-field images were obtained with a single, 3-nC micropulse, while the far-field data were averaged over 10 micropulses.

We now have demonstrated extension of the technique to the 4.5 GeV beams at CEBAF/JLAB [9] and the even more challenging task at 900 MeV at FLASH [10]. The latter is close to the ASTA case with its much lower gamma. Since the fields are reduced exponentially as $e^{-2\pi b/\gamma\lambda}$, in principle we either have to use the longer wavelengths in the

NIR or more charge integrated in the image and a more sensitive camera. Our recent modeling indicates that the FIR ODR has more photons, but it is less sensitive to the beam sizes we anticipate. The ILC-TA design-goal beam intensity [11] gives a factor of 3000 compared to APS, and the intensified or low-noise camera should give another factor of 1000. These two factors combined should allow visible to IR near-field imaging of a beam that is up to 8-10 times lower in gamma than the JLAB case, if similar impact parameters can be used. The proof-of principle of this was demonstrated at 900 MeV at FLASH/DESY in 2008 [10] in a collaborative experiment with INFN which will be summarized in a later section.

ANALYTICAL AND EXPERIMENTAL ASPECTS

ANALYTICAL MODEL CONSIDERATIONS

The basic strategy is to convert the particle–beam information into optical radiation and to take advantage of the power of imaging technology to provide two-dimensional displays of intensity information. These images can be processed for beam size information. Possible radiation sources are optical transition radiation (OTR), ODR, and optical synchrotron radiation (OSR). For completeness, the near-field ODR model as described in Ref. 7 is provided here.

The ODR is generated as the charged-particle beam passes near the metal plane. In Fig.1a below I show a schematic of the backward ODR generated from two vertical planes with a total gap of *a=2b*. This far-field representation is based on Fig. 1 of Fiorito and Rule [4]. As stated before, ODR is produced when an electron beam passes near a region where different dielectric materials are present. This is generally a vacuum-to-metal interface, and the theory [4-7] is usually for the *far-field* diffraction pattern produced by a beam passing through apertures or slits in conducting planes. In the present case, we effectively integrate over angle and frequency since our optical system is focused on the ODR source itself, i.e. the *near-field* image on the screen. Therefore we propose a simplified model of the near field based on the method of virtual quanta described by Jackson [12] in dealing with the photon-like fields of relativistic beams. One convolves the electron beam's Gaussian distribution of sizes σ_x and σ_y with the field expected from a single electron at point *P* in the metal plane. One wishes to calculate the incoherent sum of radiation from all beam particles in a pulse emitted from a given point on the ODR radiator, i.e. at $\boldsymbol{u} = \boldsymbol{P} - \boldsymbol{r}_o$, where $\boldsymbol{P}$ is the field point with respect to the origin and $\boldsymbol{r}_o$ is the position of the beam centroid with respect to the origin. The impact parameter is $\boldsymbol{b} = \boldsymbol{u} - \boldsymbol{r}$, where $\boldsymbol{r} = \boldsymbol{r}(x,y)$ denotes a position in the beam measured from the beam centroid. One then can write the differential spectral intensity as:

$$\frac{dI}{d\omega}(\mathbf{u},\omega) = \frac{1}{\pi^2}\frac{q^2}{c}\left(\frac{c}{\mathrm{v}}\right)^2 \alpha^2 N \frac{1}{\sqrt{2\pi\sigma_x{}^2}}\frac{1}{\sqrt{2\pi\sigma_y{}^2}} \times \iint dxdyK_1{}^2(\alpha b)e^{-\frac{x^2}{2\sigma_x{}^2}}e^{-\frac{y^2}{2\sigma_y{}^2}} \tag{1}$$

where ω = radiation frequency, v = particle velocity, c = speed of light, q = electron charge, N is the particle number, $\alpha = 1/\gamma\lambda$, and $K_1(\alpha b) = K_1\left(\alpha\sqrt{(u_x - x)^2 + (u_y - y)^2}\right)$ is a modified Bessel function. Since one measures light intensity I, this should be proportional to $|E_x|^2 + |E_y|^2$, resulting in the K_1^2 dependence. The incoherent photon intensity is proportional to N, the number of electrons, in contrast to the case of coherent diffraction radiation in the far infrared (FIR), which is enhanced by N^2.

The APS experiments actually started with a single plane which was inserted vertically. They evaluated the beam size parallel to the single edge. In Fig.1b I show a calculation of the signal distribution in the optical near field based on this new model for a 7-GeV beam at an impact parameter of 1.25 mm. The beam size was 1375 µm by 200 µm [7].

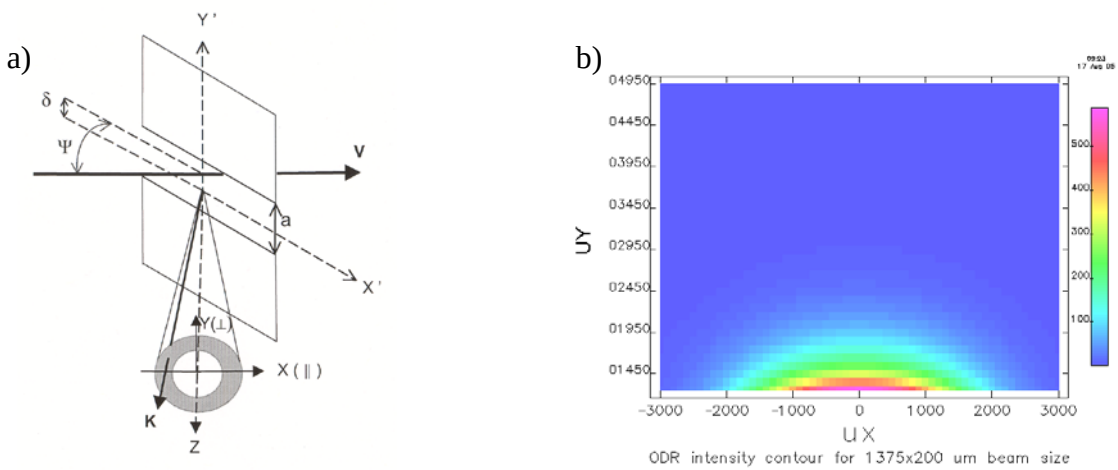

Fig. 1. a) A schematic of the backward ODR angular distribution generated as the beam passes near the metal planes and b) a calculation of the ODR light generated from a single plane for the beam sizes in the experiment at an impact parameter of 1.25 mm.

ODR MODELING RESULTS

The model has been used to evaluate beam size sensitivity for two cases for an ~ 0.5-GeV electron beam. Previously we presented results at the 20-µm level for the ILC regime [2]. For the NML case the x beam size was varied ± 20% around the 200 µm value to show the change in ODR profile. In Fig. 2 we show the ODR perpendicular polarization component for a beam size varied around 200 µm (left) and around 400 µm (right). The calculated ODR profile is of course larger than the actual beam size, but the profiles do detectably change in size with the beam size change. A 20% change in beam size from 200 µm, gives an ~ 12% change in ODR profile size.

As an additional issue we addressed the beam size sensitivity for a 400-µm beam size, but with an impact parameter of 12.5 σ_y = 5000 µm in Fig. 3. Using an 800-nm wavelength, we still calculate some sensitivity to beam size changes of 12 % in the left plot, but the 10-µm wavelength case shows very little sensitivity in its much larger horizontal profile in the right plot. It had been suggested a 14-µm wavelength could be used to increase the photon emission number in an application for protons in the Tevatron using a far-field imaging technique, but the trade is not at all favorable in our near-field

technique. So it appears that the 800-nm regime would be the better choice as has been used in far-field experiments at 680 MeV by the Frascati team using a 16-bit CCD camera [13], as well as in our more recent near-field experiment at 900 MeV using the same camera as reported at BIW08 [10].

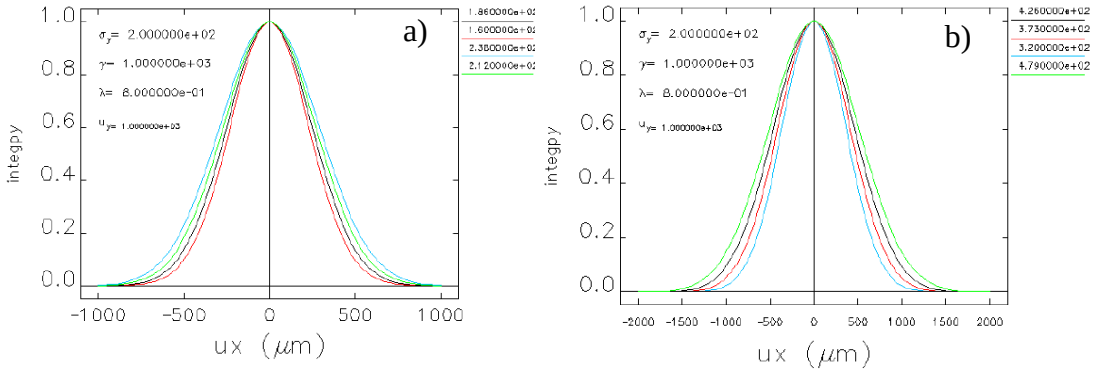

Fig. 2. Numerical results for beam size sensitivity at a) 200 µm and b) 400 µm. The impact parameter was 5 x 200 µm and gamma=1000 [10].

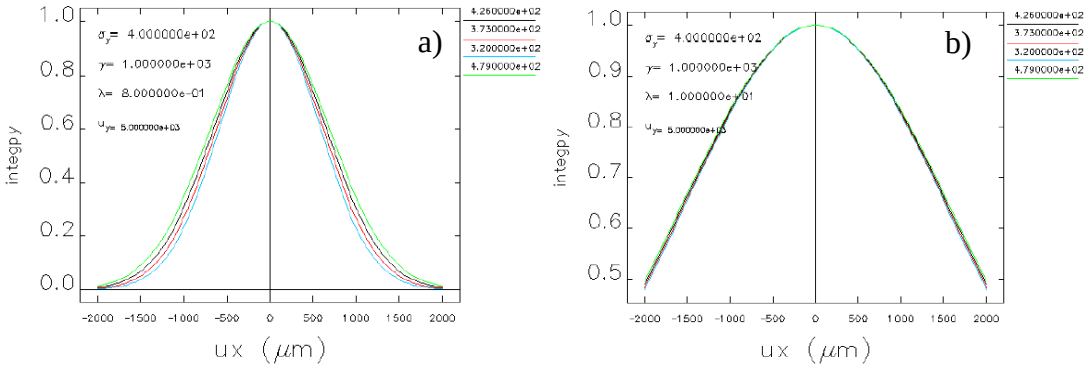

Fig. 3. Numerical results for wavelength effects on beam size sensitivity at 400 µm with a) 0.8-µm and b) 10-µm ODR. The impact parameter was 12.5 x 400 µm and gamma=1000 [10].

In general the linac is a linear device and has no bends. However, there can be some OSR emitted as the beam transits correctors, quadrupoles, the dipoles in a chicane, and the dipole for a spectrometer. These sources are generally out of focus or displaced from the ODR image position when near-field focusing is used. OTR from beam halo particles could be a background source, but if one uses an impact parameter of about 5-6 σ_p, where this is the size perpendicular to the single edge, this contribution generally should be negligible.

JLAB EXPERIMENTAL RESULTS

The test station was implemented by P. Evtushenko et al. [9] to the provided general specifications on the CEBAF Hall-A transport line as shown schematically in Fig. 4. The test station includes an OTR foil and an Aluminized Si converter screen with stepper motor control and the imaging system. The Al coatings were done at Fermilab by E. Hahn. The dipole that when powered directs the beam into this line is 8 m upstream of the ODR converter screen. A Pro-E version of the station is shown in Fig. 5 that more clearly depicts the physical appearance of the hardware and screens. The optical transport line involves two mirrors and two relay lenses enclosed in the 2-in. diameter Thorlab tubes. The camera calibration factors in x and y are 11 µm per pixel.

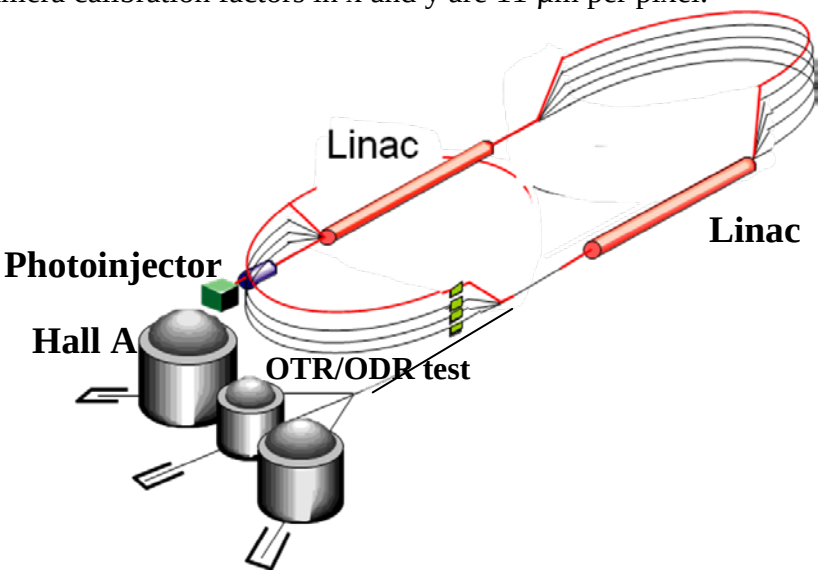

Fig. 4. A schematic of the CEBAF/JLAB recirculating linac which can provide 100 µA at 1,2,3,4, and 5 GeV and the location of the OTR/ODR test station area on the HALL A line.

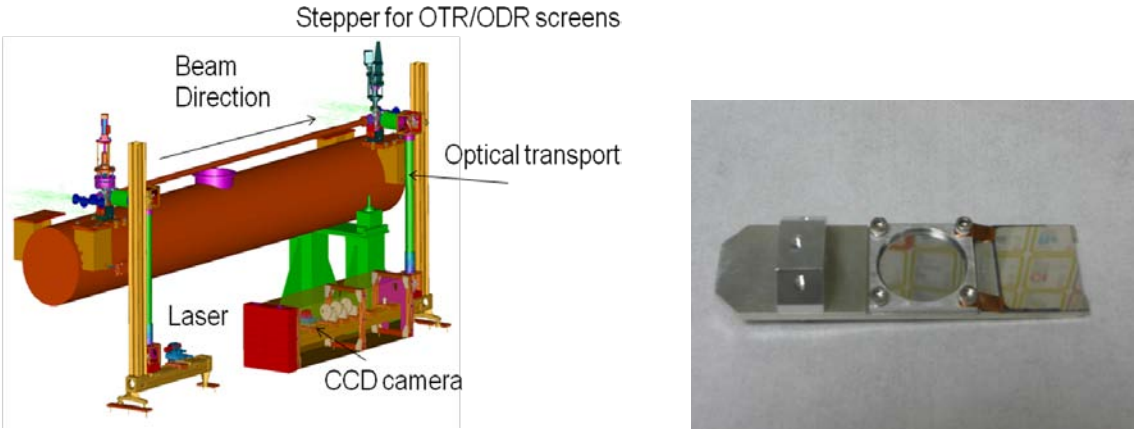

Fig. 5. A Pro-E drawing (Left) of the OTR/ODR station at JLAB showing the alignment laser, ODR assembly, optical transport, and ODR CCD camera and photograph of the OTR and the ODR converter screens (Right) [9].

In this case a standard 10-bit CCD camera was used to record the near-field (focus at the object) ODR images at the Al metal screen. Reference images were taken with OTR by inserting the Al screen into the beam and using the same optics and camera. For these conditions we found the OTR about 10 times more intense than the ODR and used a neutral density filter to prevent camera saturation with OTR.

The most fundamental results are the OTR and ODR image sizes generated by the 4.5-GeV beam as it passes through and near the metal screen, respectively. These are shown in Figs. 6and Fig. 7. The OTR images in Fig. 6 show the a) total intensity, b) horizontal polarization component and c) vertical polarization component. We see a 20-25 µm smaller beam size when using the perpendicular polarization OTR components as described previously [9].

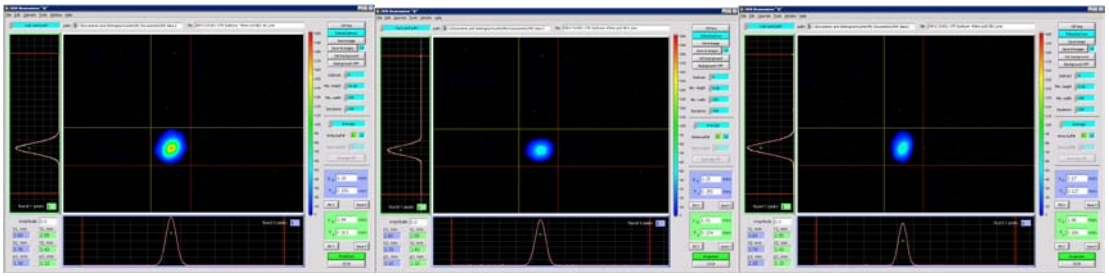

a) b) c)

Fig. 6. Results of early near-field imaging tests: the OTR images observed with a) total intensity, b) horizontal polarization, and c) vertical polarization components. The latter two show a reduced size in the perpendicular plane. Initial beam size about 150 µm by 160 µm for x and y, respectively, obtained with 5µA tune beam.

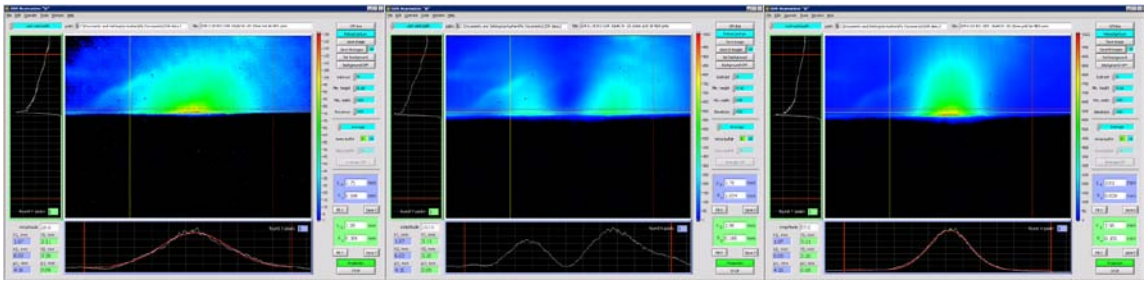

a) b) c)

Fig. 7. Results of near-field imaging tests: the ODR images observed with a) total, b) horizontal, and c) vertical polarizations for an impact parameter of 1.0 mm with the same beam size setup as Fig. 6.

Another key experimental result was obtained by using the perpendicular (vertical in this case) polarization component to assess the horizontal beam size. In this case an upstream quadrupole magnet field was scanned to vary the observed beam sizes. A comparison of the OTR image profile sizes and the ODR image sizes is shown in Fig. 8. There is a clear tracking of the beam-size effect with ODR. The ratio of sizes for ODR/OTR image size was tracked as the OTR determined beam size varied by a factor of two (as also seen in the wire scan data). The minimum OTR beam size was ~120 µm.

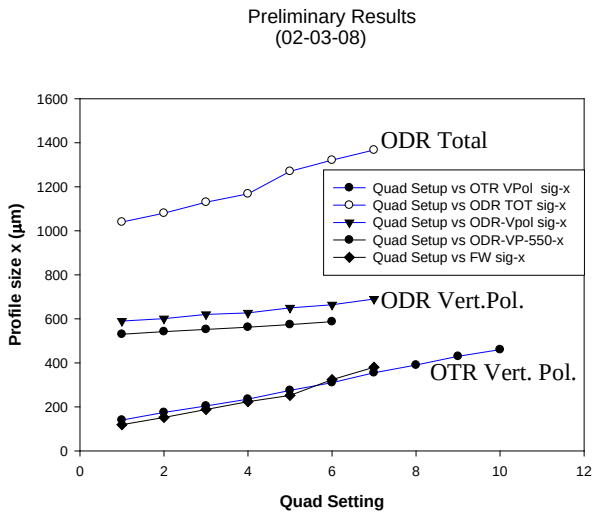

Fig. 8. The observed vertically polarized ODR and OTR image size variation with the upstream quadrupole magnet current. The beam sizes determined with a wire scanner (black line with black diamond symbol) at a nearby z location are also shown as close to that of the vertically polarized OTR (blue line with black diamond symbol).

FLASH EXPERIMENTAL RESULTS

An opportunity to test the feasibility of the near-field monitor at 900 MeV was identified in discussions with staff at FLASH in Germany and Frascati in Italy. In this case a complementary test was proposed to the ongoing far-field ODR experiments of the Frascati team [12]. The FLASH facility includes a PC rf gun, two bunch compressors, and an approximately 1 GeV SC rf linac as schematically shown in Fig. 9. The accelerator is designed to drive a soft x-ray FEL, but in addition it has ongoing programs in diagnostics developments in electro-optic sampling, a transverse rf deflector, optical replica synthesizer, and ODR. A bypass line indicated in Fig. 9 was used for the ODR tests. The converter consisted of an aluminized Si nitride wafer with a slit chemically etched of 1–mm height. A test beam with 6 bunches and 1 nC per bunch operating at 5 Hz was generated in the FLASH facility and transported to the test station. A reference OTR image as shown in Fig. 10 was obtained with the screen inserted to intercept the beam. Ultimately 10 images (60 nC integrated) were summed to improve statistics for the ODR signal obtained using an 800 x 80 nm band pass filter. The beam was positioned at the top edge of the slit, and then the actuator was stepped in 100-µm steps. An example of the image obtained with a 400-µm beam offset from the top edge is shown in Fig. 11. The dark current from the photoinjector has been subtracted from the total beam intensity. The dim ODR image is seen near both top and bottom edges. The region of interest (ROI) sampled only the top image and gave an ODR profile width of about σ_x=360 µm as shown in Fig. 11 in comparison to the original OTR-measured beam size of 205 µm.

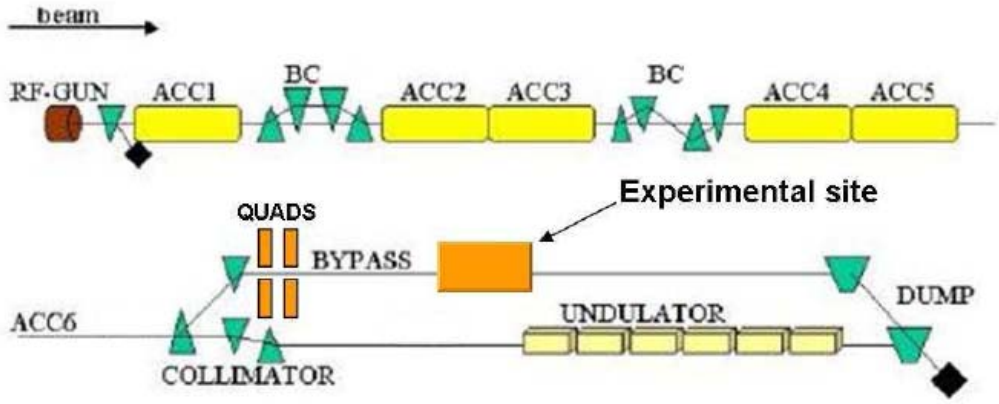

Fig. 9. Schematic of the FLASH facility with the OTR/ODR experimental site in the bypass line indicated.

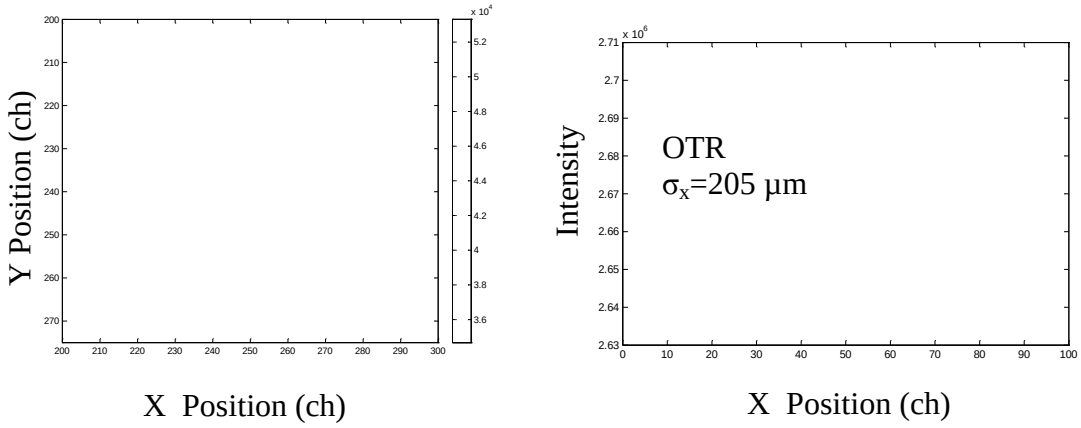

Fig. 10. Near-field OTR image (L) and x profile (R) at 900 MeV on FLASH at the test site.

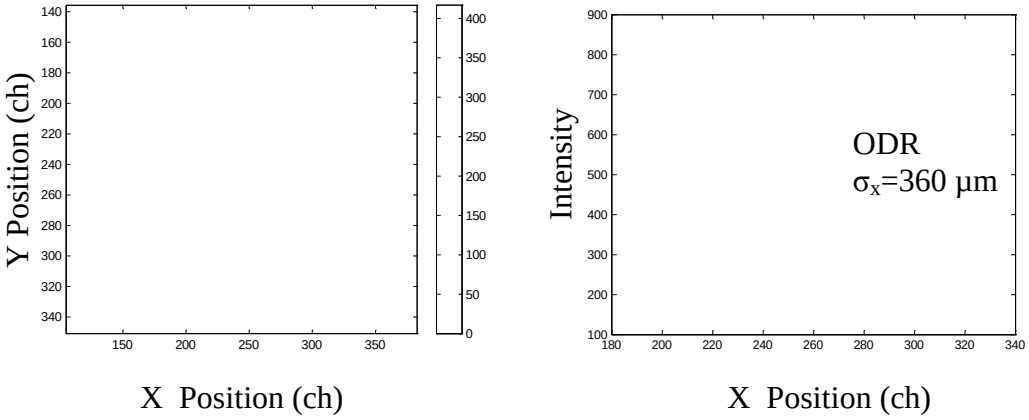

Fig. 11. Near-field ODR Image (L) and x profile (R) at 900 MeV and about 30 nC image integrated obtained at FLASH with a 16-bit camera. The actual beam size is σ_x= 205 um and the ODR image size is σ_x~360 um. The slit is 1-mm high.

With the first experimental results in the near-field at γ=1800, we performed post-experiment modeling for these specific parameters. The results of the numerical evaluations by C.-Y. Yao [10] using Eq. 1 are shown in Fig. 12. The left plot shows the total intensity profile for different impact parameters starting at 500 µm. The ODR x profile was calculated to range from 286 µm to 400 µm for impact parameters from 500 to 1200 µm for total intensity, in reasonable agreement with the experiment. The right plot shows the calculated beam-size sensitivity for the 200 µm ± 20% horizontal size. The ODR x-profile clearly tracks the changes with its roughly 30-µm change in sigma per step or 10-12% relative changes. In these cases, the dots on the curves are the ODR results and the solid lines are the Gaussian fits to those points. It is clear the Gaussian assumption is appropriate for these results.

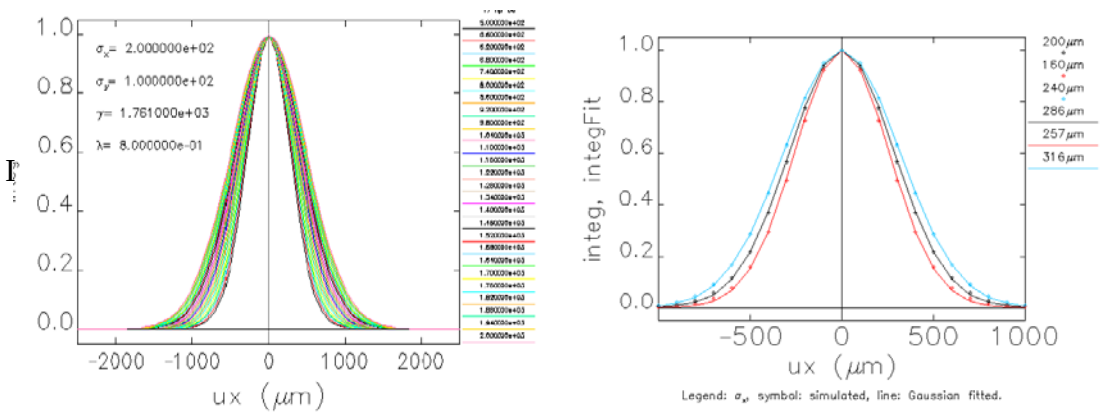

Fig. 12. Calculated near-field ODR horizontal profiles for the FLASH case with the variation of impact parameter (left) and the 20% variation of initial beam size around 200 µm (right) [10].

ASTA APPLICATION

Beam sizes for the baseline ASTA facility appear to be between the two cases calculated in Ref. 2 and above and similar to the JLAB CEBAF case in some parameters as shown in Table 1. When the emittance is indeed degraded by the bunch compression process from 4.5 to ~25 pi mm mrad and with the beta function of 2 m, one would expect beam-size sigmas of ~160 µm at 750 MeV at ASTA. From the intensity point of view, the factor of 3000 in charge combined with an assumed camera-sensitivity factor of 1000 over a standard CCD camera more than compensates for the expected reduction factor for low gamma compared to the 4.5-GeV case. (This reduction factor is about e^6 = 400 for the 1.5-GeV case so just a standard CCD camera might then be used.) Analytical assessments of beam size sensitivity for the specific low gamma conditions have been described in a previous section, but experiments are still warranted. In general, the basic OTR station with a stepper motor drive on the actuator that would allow selection of the OTR screen or ODR converter should be adequate as demonstrated at JLAB and APS. It would be preferable to have two vertical actuators with one screen inserted from the top and one from the bottom to establish a variable vertical slit height. A filter wheel or other device to select ND filters, bandpass filters, and two linear polarizers would be planned.

Table 1: Summary of the beam energy, beam sizes, current, and charge per image for APS, CEBAF, FLASH, and ASTA cases.

Parameter	APS	CEBAF	FLASH	ASTA
Energy (GeV)	7	1- 5	0.9-1	0.5-1.50
X Beam size (μm)	1300	30-50	100-200	160-300
Y Beam size (μm)	200	30-50	100-200	160-300
Current (nA)	6	100,000	1000	50,000
Charge/33 ms (nC)	3	3,000	10(test)	10,000

The camera for ODR needs to be evaluated, but an extended IR or NIR response with either a GaAs MCP intensifier and/or 16-bit capability would be needed. The almost flat response of a GaAs PC MCP out to 880 nm is shown in Fig. 13. Such an intensified CCD camera with 10-bit dynamic range would be a candidate. The previous DESY FLASH ODR results with a 680-MeV beam and an image integrated over only ~175 nC in 2 s used a 16-bit Hamamatsu camera and supports the feasibility [13] and the simple scaling technique employed. Since the latter was a far-field test, and they used a 40-nm wide bandpass filter centered at 800 nm, they exacerbated the low photon yield issue. It's not clear from their paper what their beam-size sensitivity really is in the presence of the divergence of 30 μrad, but with near-field imaging one could use a wider bandpass filter and increase the signal. Our actual proof-of-principle, near-field experiment [10] at FLASH at 900 MeV was presented in the previous section.

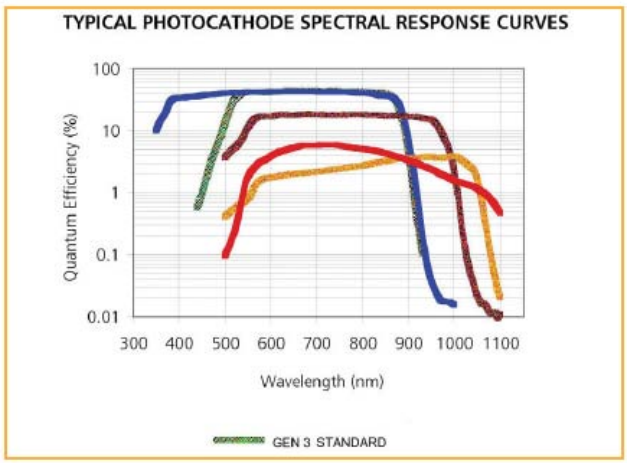

Fig. 13. The reported response of the GaAs PC MCP in the NIR for the Pulnix ICCD with a Generation 3 MCP (green curve follows the blue curve at long wavelength end).

The ODR station would be initially positioned in the "test area" and/or diagnostics section where an OTR cube could be shared as indicated in Fig. 14. In the test area, M. Church estimates he could provide beta functions varying from 0.2 m to 100 m for test purposes. Some optical transport to bring the radiation to the shielded camera would be needed. Operationally, one could consider a three-station configuration to provide an emittance monitor independent of the beta function determination. A beam waist generated at the center screen with adequate drift either way would simplify the emittance calculation. The expected beam sizes for the high-emittance case would be 520

µm and 70 µm, respectively, with about $5^{½}$ times smaller beam sizes in the low-emittance case. Far-field imaging could be evaluated for beam-size sensitivity to the dimension perpendicular to the edge [3,4,6] or a second set of orthogonal screens could be used. The reference beam sizes at ASTA would be determined at lower macropulse charge by OTR imaging with the beam directly striking the metal screen. Depending on the actual beam sizes and the screen thickness, signals from a number of micropulses at the 3 MHz rate can be integrated to assess beam size. These screens would not be inserted at full macropulse charge, but hopefully there could be a lower charge that could be used as an overlap point with the ODR data. The ODR is then generated as the charged-particle beam passes near the metal plane in the NI mode at full current.

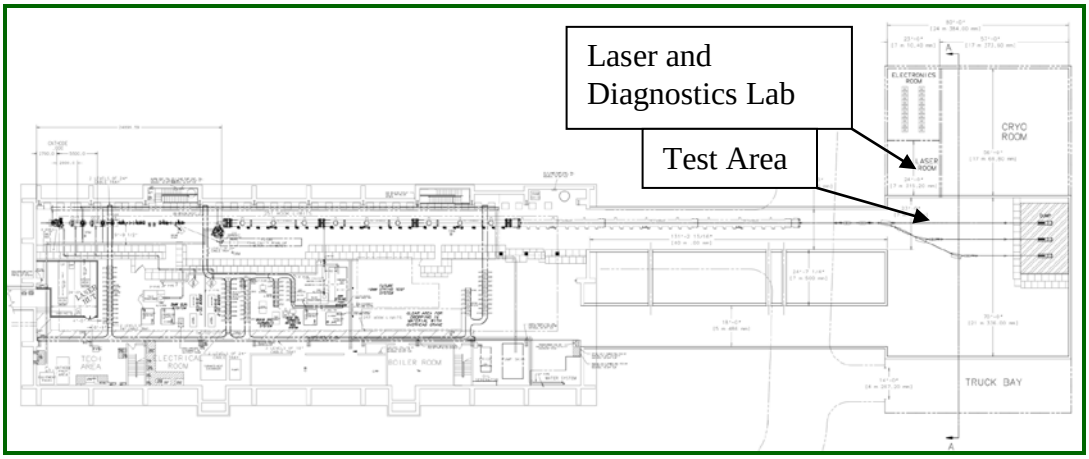

Fig.14. Schematic of the ASTA Downstream beam line with laser and diagnostic optical lab and test area indicated (courtesy of Mike Church, 12/08). Need Update.

SUMMARY

In summary, it is proposed that the ASTA diagnostics plans include the development of an ODR imaging station in the downstream beam line areas for a NI beam-size monitor. The baseline plan would be to use visible to IR/NIR imaging with a sensitive camera and share an actuator on a stepper motor with the OTR screen at that station. A double vertical actuator assembly which would allow an adjustable vertical height of the horizontal slit would be preferred for the initial tests at the test position. This would also allow far-field imaging tests to be done to evaluate beam size sensitivity in the plane perpendicular to the slit direction. Complementary and proof-of-principle tests have been done at JLAB and FLASH, respectively, in FY08. Subsequent beam tests at ASTA should help to establish the applicability of the diagnostic to other locations in the beam line where the OTR stations already exist.

ACKNOWLEDGEMENTS

The author acknowledges discussions with S. Nagaitsev, M. Church, H. Edwards, and M. Wendt on ASTA, collaborations with P. Evtushenko, A. Freyberger, and C. Lui at

JLAB, collaboration with C.-Y. Yao of ANL, and collaborations with E. Chiadroni and M. Castellano of INFN.

REFERENCES

1. Alex H. Lumpkin, "Possible ODR Imaging Diagnostics for ILCTA", talk presented at ILC-TA Workshop, Fermilab, November 28, 2006.
2. Alex H. Lumpkin,"Potential ODR Imaging Diagnostics for ILC-TA at NML", Fermilab Tech. Note, DocDB-2929-v1-2007.
3. M. Castellano, Nucl. Instrum. Methods Phys. Res. A **394**, 275 (1997).
4. R. B. Fiorito and D. W. Rule, Nucl. Instrum. Methods Phys. Res. B **173**, 67 (2001).
5. T. Muto et al., Phys. Rev. Lett. **90**(10), 104801-1 (2003).
6. P. Karataev et al., Phys. Rev. Lett. **93**, 244802 (2004).
7. A. H.Lumpkin et al., Phys. Rev. ST AB, **10** 022802 (2007).
8. A.H. Lumpkin et al., "Far-Field OTR and ODR Images Produced by 7-GeV Electron Beams at APS", proceedings of PAC07, Albuquerque, June 25-29, 2007.
9. P. Evtushenko et al., Near-field Optical Diffraction Radiation Measurements at CEBAF", Proceedings of BIW08, JACoW, 2008.
10. A.H. Lumpkin et al., "Considerations on ODR Beam-size Monitoring for Gamma=1000 Beams", Proceedings of BIW08, JACoW, 2008.
11. M. Ross, "Challenges of the Main Linac", talk at ILC School, FNAL, July 25, 2007.
12. J.D. Jackson, *Classical Electrodynamics*, (John Wiley and Sons, New York, 1975) Sec. 15.4.
13. E. Chiadroni et al., "Non-Intercepting Electron Beam Transverse Diagnostics with ODR at the DESY FLASH Facility", Proceedings of PAC07, Albuquerque, June 25-29, 2007.